Final Report

NASA NAG-3-720

UNDERSTANDING THE INTERDIFFUSION BEHAVIOR AND DETERMINING THE LONG TERM STABILITY OF TUNGSTEN FIBER REINFORCED NIOBIUM-BASE MATRIX COMPOSITE SYSTEMS

TO:

NASA-Lewis Research Center
21000 Brook Park Road
Cleveland OH 44135

BY:

John K. Tien
Principal Investigator

Columbia University
New York, New York 10027

Introduction

The initiative for reliable long-term space power generation has focussed attention on the need for high temperature structural materials. These materials must possess not only good high temperature strength and stiffness, but also long term reliability and microstructural stability. In response to this need this program addressed the long term interdiffusional stability of tungsten fiber reinforced niobium alloy composites.

The matrix alloy that is most promising for use is Nb1Zr. It is our understanding that this alloy has attractive thermal and strength characteristics but long term creep resistance and stiffness are inadequate. Thus the incorporation of the highly creep resistant and stiff ST300 thoriated tungsten fibers into a Nb1Zr matrix might yield a suitable material. However, whenever one places two dissimilar materials together at elevated temperatures interdiffusion and, in some cases, solid state reactions, can occur. In the case of the W/Nb system, interphase formation is not an issue; W and Nb are totally miscible. Thus, only interdiffusion and the associated recrystallization of the heavily worked ST300 fibers are concerns for long term reliability of W / Nb1Zr composites.

As an ancillary project to this program, efforts were made to assess the nature and kinetics of interphase reactions between selected beryllide intermetallics and nickel and iron aluminides. Beryllides are very high melting point intermetallics with extremely low densities. In addition to having extremely low densities and high melting points, beryllides offer the unique opportunity to very nearly match the coefficients of thermal expansion (CTE) of proposed nickel aluminide and iron aluminide matrices. Being intermetallic in nature, one may expect beryllide fibers to have several properties that are considerably more attractive than the corresponding properties of ceramic, including graphite,

fibers. From a composite processing standpoint, the wettablity of intermetallics to metals and, presumably other intermetallics, is generally far superior to ceramics. Additionally, this often also translates in only marginal fiber / matrix bonding and load transfer characteristics. It may also be expected that intermetallic fibers, including the low symmetry beryllides, will have superior handlability as a result of lower defect sensitivity, higher toughness, and higher strain to failure. However, as stated above for W / Nb composites, one of the primary concerns for any high temperature composite is the nature and kinetics of fiber / matrix interactions.

W / Nb1Zr Composites

In order to assess the interdiffusional kinetics for the W-fiber / Nb1Zr system a simple model was chosen. Since only 1% Zr is present in the matrix material, planar diffusion couples of elemental W and Nb were chosen. The choice of planar geometry diffusion couples was made so that kinetic data in the form of composition and temperature diffusion coefficients could be obtained. The temperature range chosen was from 1500K to 1800K. Both planar geometry diffusion couples and 40 volume % 218CS (non-thoriated W fiber) reinforced Nb were annealed for times between 100 and 500 hours. The diffusion couples and composite panels used in this study were fabricated by NASA-Lewis. The planar geometry diffusion couples were HIP'ed and the composites were fabricated by NASA-Lewis' Arc-spray technique. The annealed specimens were subsequently mounted and metallographically prepared. Composition - position profiles were determined for the specimens by energy dispersive spectroscopy (EDS). The SEM / EDS profiles were obtained using a Joel 35C scanning electron microscope equiped with a PGT

System 3 EDS unit. Spectrums were taken at 1 micron intervals across the interface using an electron accelerating potential of 25 kV. Elemental concentrations were determined using PGT's BSAM standard analysis software which compares obtained spectra to spectra of high purity elemental standards.

Interdiffusion coefficients were obtained using the time honored Boltzman-Matano analysis. This method is a graphical (numerical) solution to Fick's second law for diffusion when planar interface and infinite media boundary conditions are maintained. The Boltzman-Matano solution is expressed as:

$$\tilde{D}(C) = \frac{-1}{2t}\left[\frac{dc}{dx}\right]^{-1}\int_{C_o}^{C} x\,dC' \qquad \text{Eqn. 1}$$

where D(C) is the diffusion coefficient, C is the composition, t is the diffusion time and x is the position relative the the Matano interface (the zero-flux plane). The experimentally determined interdiffusion coefficients are shown in figure 1. Due to competing nature of the slope and integral in the numerical solution, calculated coefficients near the terminal compositions are invalid and have been deleted. For the purpose of the work discussed below, diffusivities near the terminal compositions found by extrapolating to these compositions. These experimentally determined interdiffusion coefficients were compared to values that were extrapolated down arrheniusly from the higher temperature data of Hehemann and Leber [1]. As seen in figure 2, significant variation was found between the extrapolated and experimental values. For both 1500K and 1800K the extrapolated diffusivities underestimate the experimental values, with increasing divergence as temperature is further reduced. Also, this divergence was seen to be most pronounced at the W-rich concentrations. The

experimentally determined diffusivities were also compared to data contained in a Westinghouse internal report and were found to be generally consistent with the Westinghouse data taken under similar conditions [2].

Having determined the interdiffusion coefficients for the temperatures of interest, composition profiles were calculated using numerical solutions to Fick's second law (Eqn. 2) This finite difference computer code, which was

$$\frac{dC}{dt} = \frac{1}{r^n}\frac{d}{dr}\left[r^n \tilde{D}(C,T) \frac{dC}{dr} \right] \qquad \text{Eqn. 2}$$

adapted from the program of Tenney and Unnam [3], calculates diffusion profiles for diffusion couples with planar, cylindrical, or spherical geometry with finite boundary conditions. Using both the experimentally determined and extrapolated diffusivities, diffusion profiles were calculated to emulate the diffusion couples and composites annealed in this study. Considerably better agreement was found when using the values determined in this study. As an example of the agreement between observed and calculated profiles, see figure 3.

Having obtained a reasonable degree of confidence in our ability to predict composition profiles for short term high temperature exposures, efforts were made to forecast the level of interdiffusion for W / Nb composites for very long term exposures. For this effort, the ability of the numerical solutions utilized to handle finite boundary conditions (i.e., overlapping diffusion fields) was crucial. Figure 4 illustrates radial diffusion profiles for a 40 volume percent 200 micron diameter fiber reinforced composite annealed from 1 month to 10 years. Clearly, significant degradation of fiber properties can be expected at the very long times.

It must be noted that a great deal of care in necessary in determining diffusion coefficients. Often accuracy in determining these coefficients is limited to within a factor of 2 or 3. This uncertainty can lead to large systematic errors when predicting composition profiles for very long times. Therefore, it is crucial that all possible precautions be taken to insure the accuracy of the interdiffusion coefficients used for these predictions.

Beryllide / Aluminide Composites

For this portion of the program, four candidate beryllide reinforcements were chosen for study. These included $TiBe_{12}$, $ZrBe_{13}$, Nb_2Be_{17}, and Ta_2Be_{17}. Matrix materials included stoicheometric NiAl without significant alloying additions and the off-stoicheometry Fe-40%Al binary intermetallic. Composite samples provided by NASA-Lewis were fabricated by embedding a bar of the individual beryllide materials (approximately 3.2 mm x 3.2 mm in cross-section) in the aluminides using a powder metallurgical technique with pre-alloyed powder. After consolidation individual specimens from each of the composites were vacuum annealed for times ranging from 10 hours to 500 hours Annealing temperatures used were 1200K and 1300K. The annealed specimens were subsequently mounted and metallographically prepared in order to observe details at the fiber / matrix interface in cross-section. Annealing and specimen preparation were done by NASA-Lewis and Brush-Wellman.

Composition - position profiles were determined for the specimens by two methods: energy dispersive spectroscopy (EDS) and scanning Auger microscopy (SAM). The SEM / EDS profiles were obtained using a Joel 35C scanning electron microscope equiped with a PGT System 3 EDS unit.

Spectrums were taken at 1 mm intervals across the fiber / matrix interface using an electron accelerating potential of 25 kV. Elemental concentrations were determined using PGT's BSAM standard analysis software which compares obtained spectra to spectra of high purity elemental standards. The determination of beryllium content was determined by subtraction from 100% because this unit's inability to detect light elements, such as beryllium. SAM profiles were determined in an analogous manner using a Phi SAM 590 scanning Auger microscope. After initially sputtering the sample surface to remove surface contamination, spectra were taken at known intervals across the beryllide / aluminide interface. Elemental concentrations were calculated using the relative peak height intensities as per Equation 3 [4]:

$$C_x = (I_x / S_x D_x) / \Sigma_a (I_a / S_a D_a) \qquad \text{Eqn. 3}$$

where C_x is the concentration (atomic fraction) of element x, I_x is the peak-to-peak amplitude of the derivative of the Auger electron distribution function (dN(E)/dE) at element x's characteristic energy, S_x is element x's sensitivity factor, and D_x is the instrumental parameter for element x. Beryllium concentrations were determined by summing the Be and BeO peaks. The persistence of significant levels of BeO on the specimen surface, even after relatively long sputtering times, is believed to be the result of the metallographic polishing procedures used.

Very good agreement was found between the composition - position profiles obtained for identical specimens by EDS and SAM. For this reason it is believed that the elemental subtraction method used for the EDS profiles and peak summation method used for the SAM profiles are valid for determining

beryllium concentrations. As a result, composition - position profiles taken by both methods were used interchangeably in the sample analyses.

In all samples examined, a reaction zone phase formed at the beryllide / aluminide interface during the fabrication process. For all of the samples this reaction zone consisted of two distinct phases in a dual layer structure. This is typified by the Nb_2Be_{17} / NiAl reaction zone shown in figure 5. Despite the initial similarity of the various beryllide / aluminide interface structures, kinetic analyses revealed what are believed to be three distinct classes of kinetic behavior for the systems studied.

A. The Nb_2Be_{17} / NiAl System.

The Nb_2Be_{17} / NiAl system was unique among the systems studied in that it exhibited classical interface control of the reaction zone evolution (i.e., linear growth or dissolution with time). In fact, the sum of the two reaction zone thicknesses decreased with time at temperature. An analysis of the evolution of the individual phases in the reaction zone showed that the phase immediately adjacent to the beryllide grew linearly with time at the expense of the phase adjacent to the aluminide. This is illustrated in Figure 6. Therefore it appears that this shrinking phase is not thermodynamically stable at the annealing temperatures studied despite its assumed stability at the higher temperature (and perhaps pressure) processing conditions.

B. The $TiBe_{12}$, $ZrBe_{13}$, and Ta_2Be_{17} / NiAl Systems.

Unlike the Nb_2Be_{17} / NiAl system, these systems exhibited an initial period of of parabolic growth (i.e., long range diffusion controlled) that slowed after a period of time (See Figure 7). As previously reported, one of the reaction zone phases in the $TiBe_{12}$ / NiAl system has been identified as $NiAlBe_2$ [5].

Additionally, in this $NiAlBe_2$ phase in the $TiBe_{12}$ / NiAl system, small particles on the order of 1 to 3 mm in diameter. Although these particles were seen to coarsen somewhat with time at temperature, there volume fraction apparently remained constant. It is also interesting to note that the second phase in this system appears not to grow or shrink with annealing time, maintaining a relatively thin 1 to 3 mm in thickness. Although neither this nor the precipitates have been satisfactorily identified, limited data suggests that they may share similar compositions.

Although the kinetic behavior of the $ZrBe_{13}$/NiAl and Ta_2Be_{17} / NiAl systems were similar to that of the $TiBe_{12}$ / NiAl system, there were some distinct differences. In these systems, the reaction zone is comprised of two distinct layers that both grow parabolically with time. Phases identification has not yet been accomplished. Also, precipitates as above were not observed in the reaction zone phases.

The reason for the observed deviation from parabolic behavior for these systems is not clear, but experimental artifacts may provide some explanation. In every sample significant interaction between the beryllide and aluminide occurred during fabrication of the composite. Thus, a complex interface structure in the process of equilibrating at the higher processing temperature and pressure was in place prior to the annealing experiments. This may have resulted in the composite behaving very differently than the classical experiment of a strict binary interface reacting under high temperature exposure. As a consequence, the observed deviation from a parabolic time law may be due, at least in part, to these experimental conditions.

C. The $TiBe_{12}$, $ZrBe_{13}$, Ta_2Be_{17}, and Nb_2Be_{17} / Fe-40%Al Systems.

In each of these four Fe-40%Al systems, similar reaction zone evolution was observed. This behavior took the form of a decreasing rate of growth from the initially observed parabolic rate law. A reaction zone thickness versus $t^{1/2}$ plot for the $ZrBe_{13}$ / Fe-40%Al system is shown as an example in Figure 8. The shape of this plot, as well as the other beryllide / Fe-40%Al plots, implies that some mechanism is operating that increasingly retards diffusion across the reaction zone as annealing time increases.

Examination of the composition - position plots for these systems has revealed some very interesting phenomena that are believed to account for this decrease in reaction zone growth kinetics. Again as a typical example, the plot for the $ZrBe_{13}$ / Fe-40%Al system is shown in Figure 9. The most striking features of these plots are the concentrations of beryllium and aluminium from the terminal phases through the reaction zone phases. For both these elements, concentration drops in the the immediately adjacent reaction zone phase from the element rich terminal phase, climbs in the second and more distant phase, then drops to zero in the opposite terminal phase. In the case of the aluminum profile, the aluminum concentration in the reaction zone phase adjacent to the aluminide drops below detection limits for both EDS and SAM. This phase has been identified as $FeBe_5$. The other phase for these systems have yet to be identified.

Based on these diffusion profiles that were obtained, a "diffusion lock" mechanism is believed to have been formed in these Fe-40%Al systems. It is proposed that this locking mechanism operates because a normally mobile species, in this case aluminum, is barred from passing through the newly formed $FeBe_5$ phase. Although no ternary data exists for the Fe-Be-Al system, apparently $FeBe_5$ has no, or at most trace, solubility for aluminum, and thus

locks its further diffusion. The aluminum present on the beryllide side of the $FeBe_5$ is believed to have diffused there early on in the fabrication process, prior to the phase's formation.

A second aspect of this diffusion lock that may contribute to its effectiveness is the "uphill" diffusion necessary for the beryllium to diffuse from the reaction zone phase adjacent to the beryllide into the $FeBe_5$ phase. It is possible that the longer term, slow growth may be a result of the reaction zone phases picking up their needed elements from the relatively small amounts that diffused into the terminal phases adjacent to them early on in the fabrication process. Thus, the $FeBe_5$ may be getting the necessary beryllium from the Fe-40%Al, for example.

Of course, diffusion follows activity gradients, not necessarily concentration gradients. However, these often follow one another and, given the observed behavior, it appears that for these systems the uphill gradients at the interface between the two reaction zone phases and the "zero" aluminum solubility $FeBe_5$ phase have formed a lock that will effectively halt or drastically limit further interdiffusion and reaction zone growth.

Conclusions

Efforts on forecasting the long term behavior of tungsten fiber reinforced Nb1Zr have shown that significant interdiffusional penetration will occur in the periods between one and ten years. Although we are generally confident in the validity of this approach, we emphasize again the relative ease at which significant error can be inadvertently introduced if relatively small errors in the input diffusivities are not kept to an absolute minimum.

The specimens used in the beryllide / aluminide portion of this study unfortunately had the complication of initial phases present that may or may not

be in thermodynamic equilibrium at the annealing temperatures. As a result, some restraint is called for in interpreting the kinetic data for these samples. In spite of this limitation, however, when the composition profile data is combined with the kinetic data for the Fe-40%Al matrix systems, there is sufficient reason to believe that a diffusion lock is indeed operating.

Publications

1. M.W. Kopp and J.K. Tien, Interdiffusional Instability in High Temperature Metal Matrix Composites, Proc. 9th Riso Int. Symp., 1988, Riso National Laboratory, Roskilde, Denmark, 427-32.

2. M.W. Kopp, J.K. Tien, and D.W. Petrasek, Reaction Kinetics Between Fiber and Matrix Components in Metal Matrix Composites, Superalloys 1988, TMS, Warrendale, PA, 1988, 193-201.

3. A.J. Carbone, M.W. Kopp, J.K. Tien, S.S. Lin, H.L. Marcus, and S.L. Draper, Scripta Metall., 1988, vol. 22, pp. 1903-6.

4. J.K. Tien, M.W. Kopp, A.J. Carbone, and R.S. Bellows, Devolopment of High Temperature Composites with Long Term Stability: Intermetallics and Diffusion Barriers, Proc. Industry-University Advanced Materials Conf. II, AMI, Golden, CO, 1989, 74-82.

5. M.W. Kopp and J.K. Tien, The Kinetics of Fiber / Matrix Interactions in High Temperature Metal Matrix Composites, Proc. Industry-University Advanced Materials Conf. II, AMI, Golden, CO, 1989, 83-91.

6. J.K. Tien and M.W. Kopp, Interfacial Reactions in High Temperature Metallic and Intermetallic Matrix Composites: A Status Review, Metal & Ceramic Matrix Composites: Processing, Modeling & Mechanical Behavior, R.B. Bhagat et. al. eds., TMS, Warrendale, PA, 1990, 443-56.

7. M.W. Kopp, A.J. Carbone, and J.K. Tien, Interdiffusion and Interfacial Reactions in Beryllide Reinforced Nickel Aluminide and Iron Aluminide Intermetallic Matrix Composites, to be submitted to Met. Trans. A.

Sponsored Theses

1. M.W. Kopp, Long Term Interdiffusional Behavior in Tungsten Fiber Reinforced Niobium-base Matrix Composites, Masters Thesis, Columbia University, 1987.

2. A.J. Carbone, Interdiffusion Effects in Beryllide Reinforced Aluminide Composites, Masters Thesis, Columbia University, 1989.

References

1. R.F. Hehemann and S. Leber, Trans. AIME, 236, 1966.

2. F.G. Arcella, NASA CR-134490, 1974.

3. D.R. Tenney and J. Unnam, NASA TM-78636, 1978.

4. L.E. Davis, N.C. MacDonald, P.W. Palmberg, G.E. Riach, ad R.E. Webster: Handbood of Auger Electron Spectroscopy, 2nd Ed., Perkin Elmer Corporation, Eden Prairie MN, p. 9.

5. A.J. Carbone, M.W. Kopp, J.K. Tien, S.S. Lin, H.L. Marcus, and S.L. Draper, Scripta Metall., 1988, vol. 22, pp. 1903-6.

Figure1. Experimental Diffusion Coefficients for W /Nb at 1500K and 1800K.

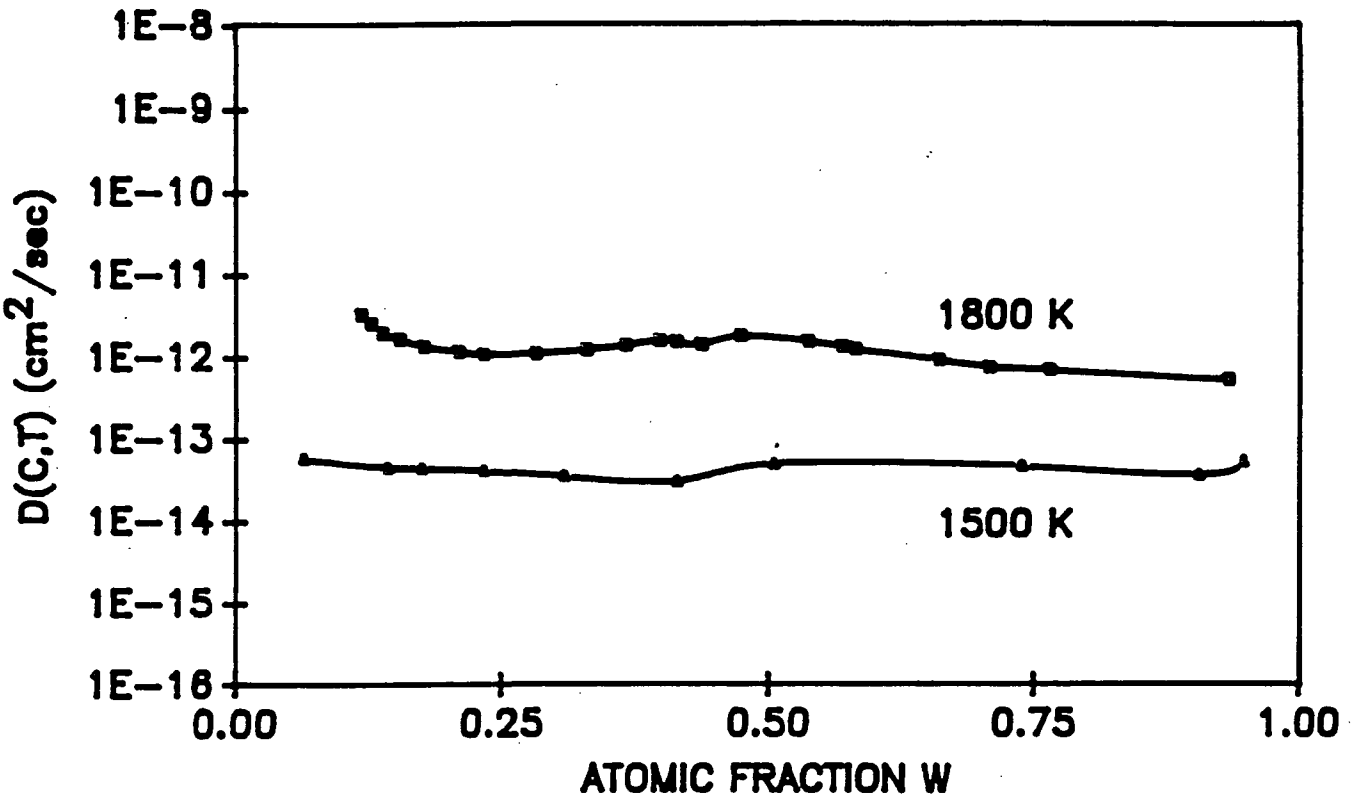

Figure 2. Log D vs 1/T for 20% W
(boxed data is extraploation)

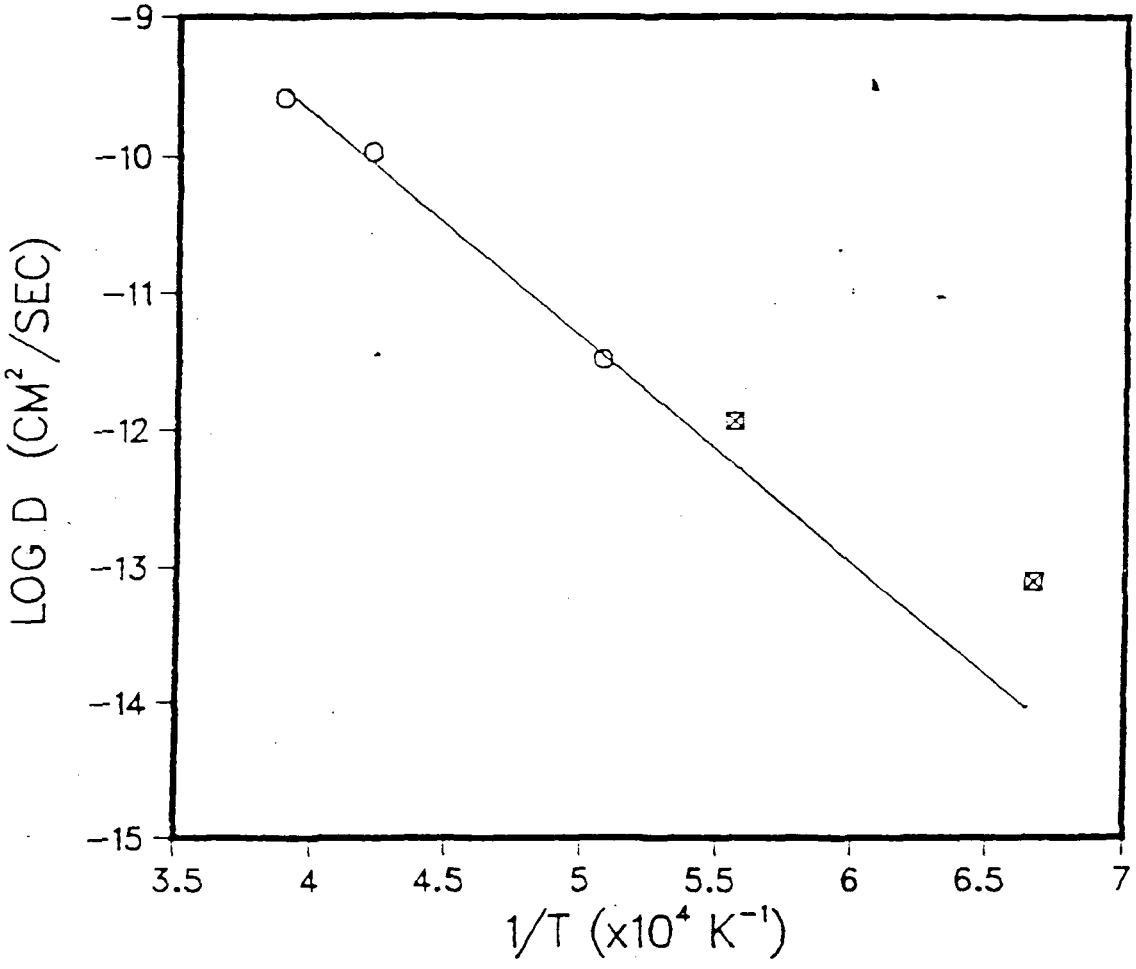

Figure 3. Experimental and calculated composition profiles for a W/Nb composite annealed at 1500K for 500 hours.

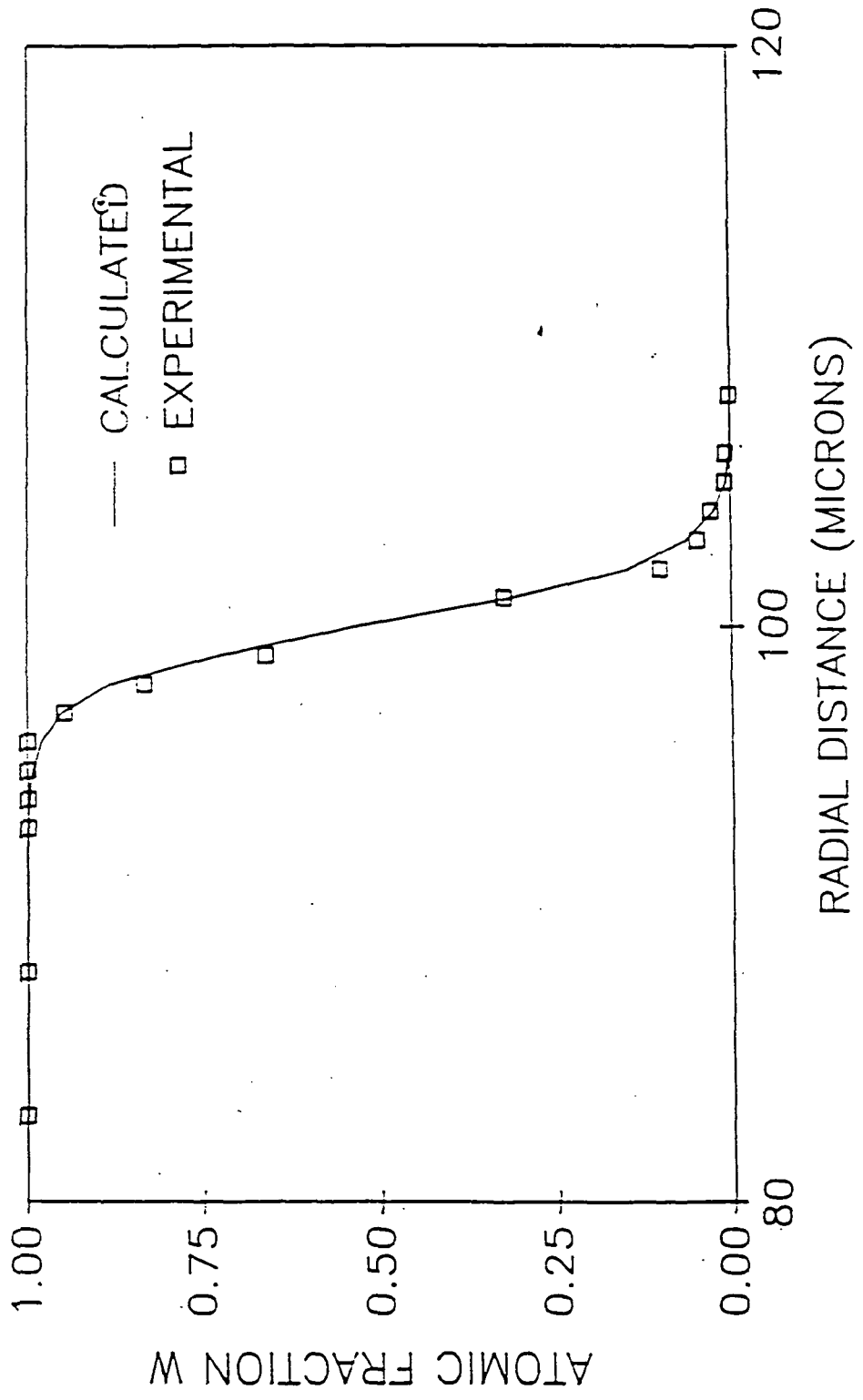

Figure 4. Long term predictions of composition profiles for a W / Nb composite annealed at 1500K.

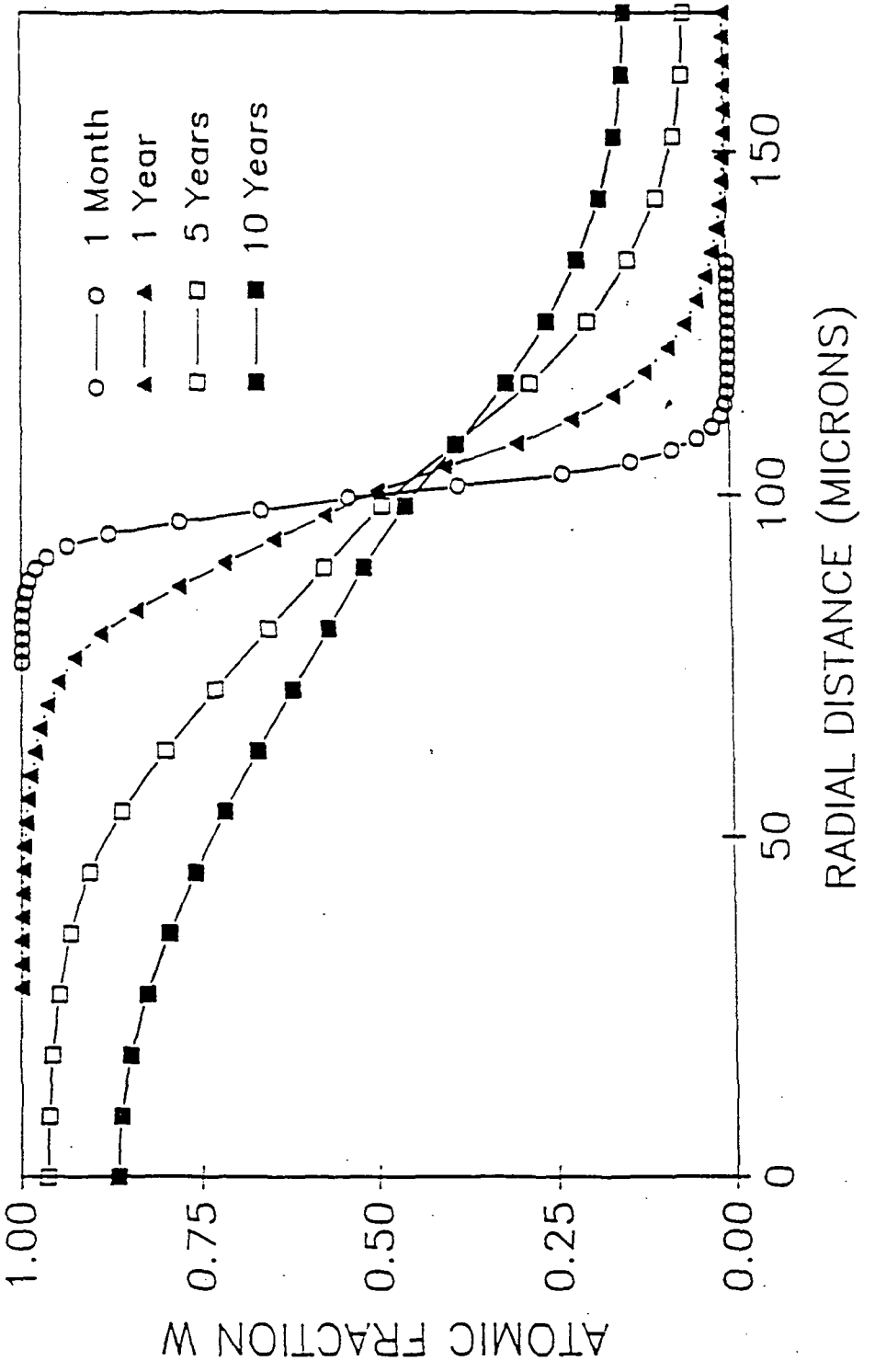

Figure 5. Reaction zone of Nb_2Be_{17} / NiAl after 25 hours at1300K.

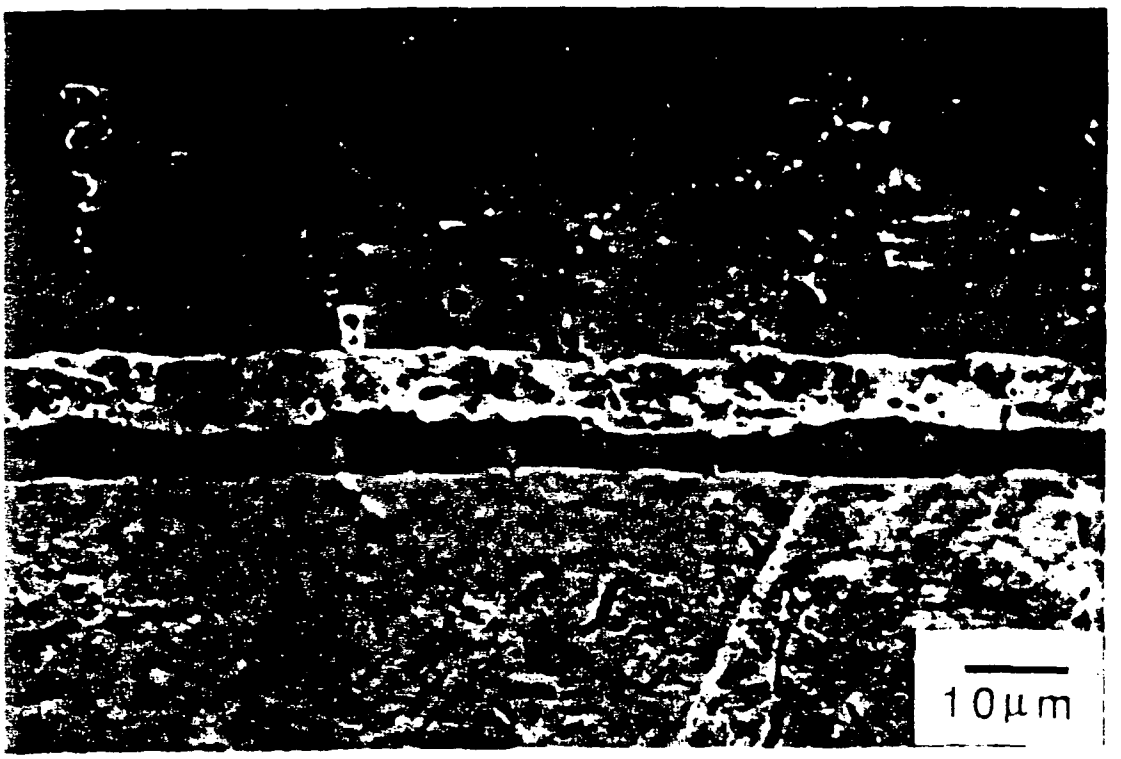

Figure 6. Reaction zone growth of Nb_2Be_{17} / NiAl at 1300K. (RZ=Total, FRZ=Fiber component, MRZ=Matrix component)

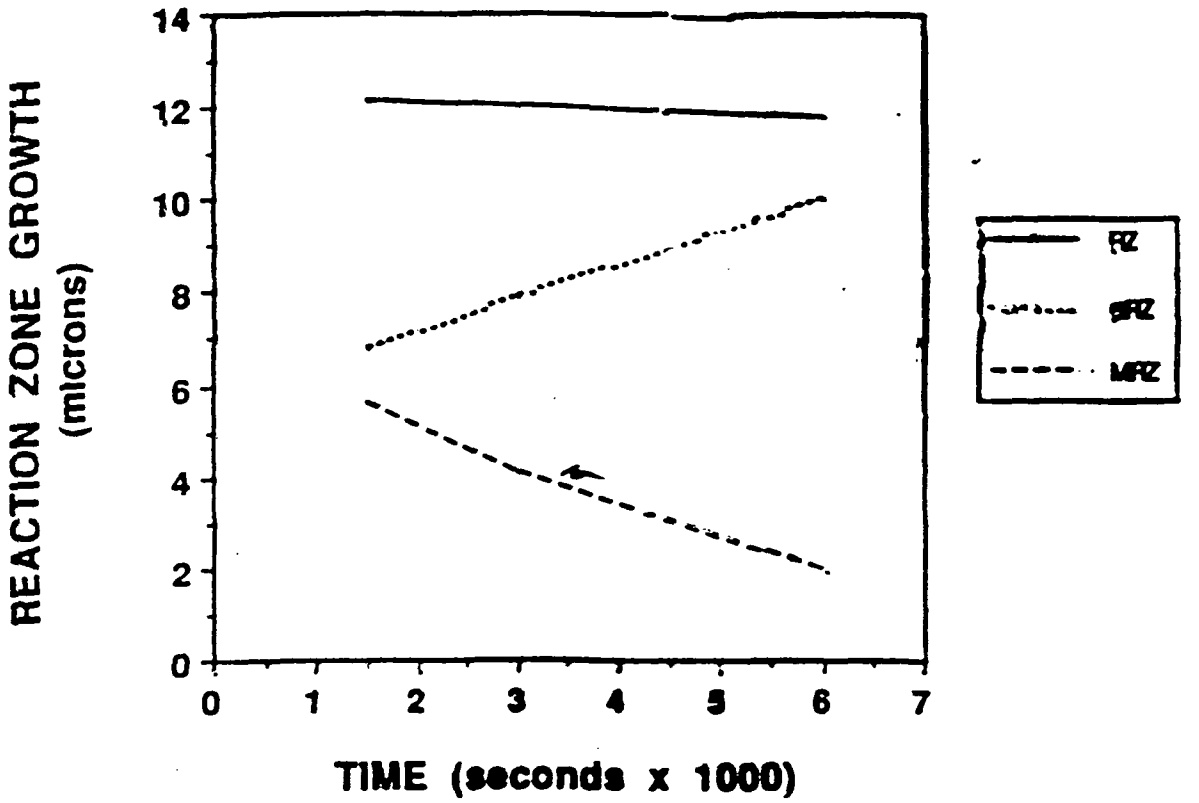

Figure 7. Reaction zone growth of $TiBe_{12}$ / NiAl.

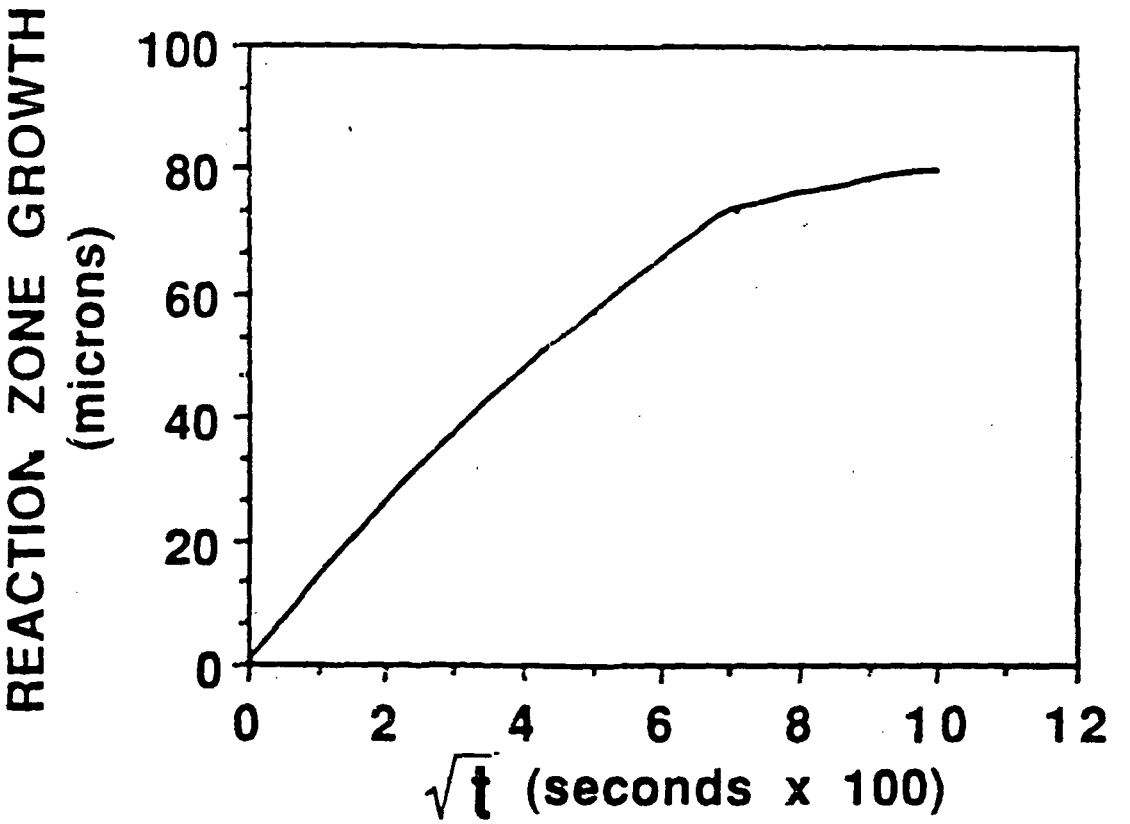

Figure 8. Reaction zone growth of $ZrBe_{13}$ / Fe40Al.

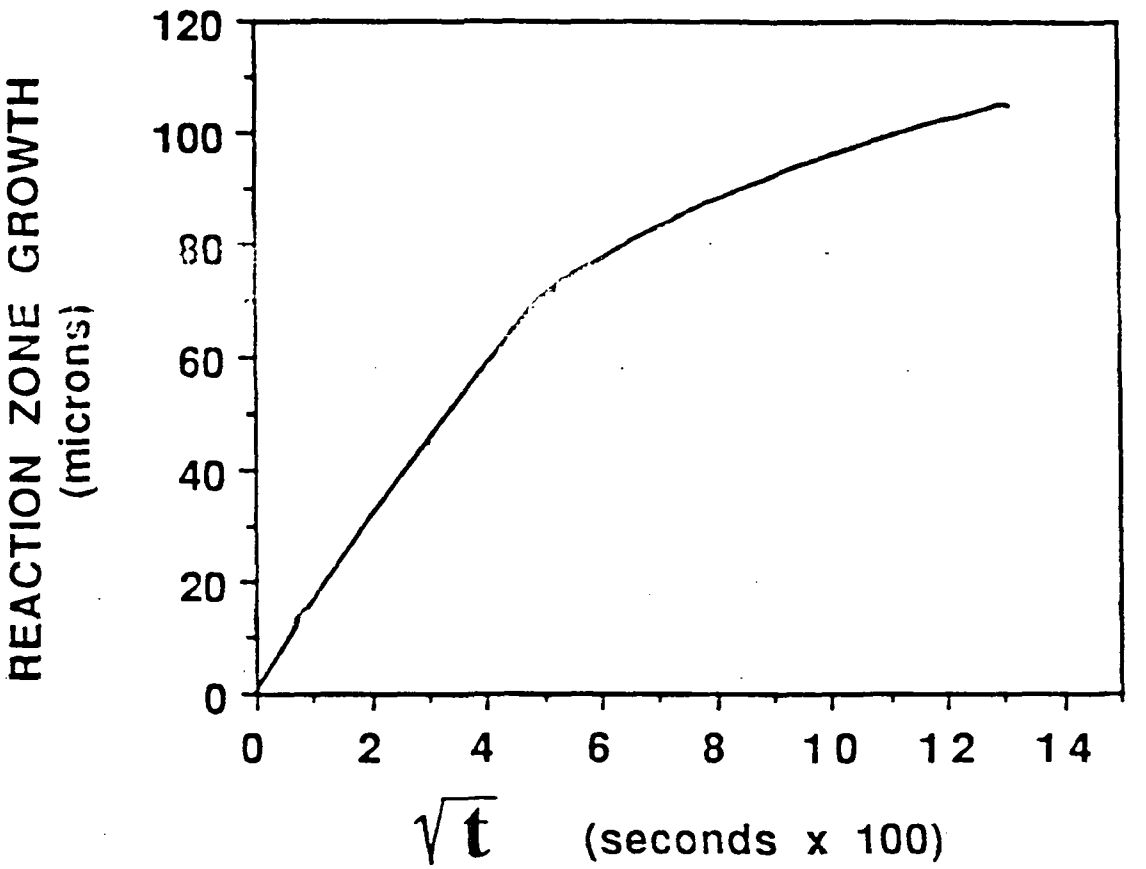

Figure 8. Composition profile of $ZrBe_{13}$ / Fe40Al.